AIP | Journal of Applied Physics

# Hydrogen stability in hydrogenated amorphous carbon films with polymer-like and diamond-like structure

J. G. Buijnsters, R. Gago, A. Redondo-Cubero, and I. Jiménez

Citation: J. Appl. Phys. **112**, 093502 (2012); doi: 10.1063/1.4764001
View online: http://dx.doi.org/10.1063/1.4764001
View Table of Contents: http://jap.aip.org/resource/1/JAPIAU/v112/i9
Published by the American Institute of Physics.

# Hydrogen stability in hydrogenated amorphous carbon films with polymer-like and diamond-like structure

J. G. Buijnsters,[1,a)] R. Gago,[2] A. Redondo-Cubero,[3] and I. Jiménez[2]
[1]*Department of Metallurgy and Materials Engineering, KU Leuven, B-3001 Leuven, Belgium*
[2]*Instituto de Ciencia de Materiales de Madrid, Consejo Superior de Investigaciones Científicas, E-28049 Madrid, Spain*
[3]*Instituto Tecnológico e Nuclear, Instituto Superior Técnico, Universidade Técnica de Lisboa, 2686-953 Sacavém, Portugal*

(Received 27 June 2012; accepted 3 October 2012; published online 2 November 2012)

Hydrogen (H) stability in hydrogenated amorphous carbon (a-C:H) films with different structures grown by (biased) electron-cyclotron-resonance chemical vapor deposition has been studied against thermal annealing and swift-ion impact (2 MeV $He^+$). For this purpose, a-C:H films with either polymer-like (PLCH) or diamond-like (DLCH) character grown on grounded or biased (−200 V) substrates, respectively, were annealed up to 450 °C. The local-order structural evolution around C sites was analyzed by x-ray absorption near-edge spectroscopy (XANES) and the H content and radiation-induced release were determined by successive elastic recoil detection analysis (ERDA) acquisitions. A relatively high H content is measured for both as-grown PLCH (∼45 at. %) and DLCH films (∼33 at. %). Upon annealing, PLCH films suffer thermal-induced surface decomposition resulting in a thickness reduction and only above 350 °C the H content in the film matrix decreases. PLCH films also display a pronounced H loss rate during ERDA measurements, whereas H is stable in DLCH. These results indicate that H bonding differs in both structures (i.e., weaker C-H bonds in PLCH). XANES shows that upon annealing both structures suffer H loss at the near surface region together with a graphitization process, although the impact is more pronounced in PLCH. XANES fine-structure reveals that aromatic clusters are formed upon annealing in PLCH due to H loss, whereas this process is partially inhibited in DLCH due to the thermal stability of the C-H bonds. © *2012 American Institute of Physics*. [http://dx.doi.org/10.1063/1.4764001]

## I. INTRODUCTION

Carbon is the building block of numerous key engineering materials possessing exceptional properties, such as diamond, graphene, carbon nanotubes, and various carbides. In addition, many amorphous carbon (a-C) thin films present high hardness, high wear resistance, low friction, and strong corrosion resistance, being appropriate as protective layers on magnetic discs, bearings, gears and engine components such as pistons and fuel injection systems.[1–3] The bonding structure of such films is characterized by the presence of $sp^3$ and $sp^2$ C hybrids with tetrahedral or trigonal coordination, respectively, as well as the incorporation of H in hydrogenated films (a-C:H). Based on the relative percentage of these $sp^3$-C and $sp^2$-C bonds and the amount of bonded H within the film microstructure, four types of a-C:H materials have been distinguished,[4] i.e., polymer-like (PLCH), graphite-like (GLCH), diamond-like (DLCH or DLC), and tetrahedral (TACH). PLCH displays the highest H content and its polymer-like structure, governed by the H terminated $sp^3$ bonds, results in a low density and soft matrix. GLCH combines low H content and high $sp^2$ content. TACH films have a relatively low H content (25–30 at. %) and a large $sp^3$-C content, whereas the content of $sp^3$-C in DLC films can vary significantly as a result of the varying content of atomic hydrogen present in the film matrix. The Young's modulus and density of DLC films are generally much lower than those of TACH films. Within the class of DLC coatings, the bonding structure and composition can vary largely depending on the applied source gases as well as on the deposition techniques and growth conditions. As a result, the mechanical and tribological properties of DLC films differ substantially from one to another.[5,6]

The ion energy of bombarding particles during growth is a crucial factor in plasma processed a-C:H films. The ion-(sub)surface interactions such as the dangling bond formation, sputtering, atomic displacement, and hydrogen depletion are strongly depending on the ion energy.[7,8] The application of a radio frequency or direct-current (DC) substrate bias voltage allows the control of the energy of the ions bombarding the surface. Thus, the substrate bias can be regarded as a decisive parameter controlling the composition, structure, physical and chemical properties and even surface morphology[9,10] of the deposited a-C:H films. Equally, the carbon bonding structure, the hydrogen content as well as the size distribution and volume fraction of voids in a-C:H films are correlating characteristics that determine the mechanical properties of these materials.[11]

The characteristics of a-C:H and DLC in particular are attractive for numerous industrial applications, including mechanical face seals, razor blades, magnetic hard discs, critical

a)Author to whom correspondence should be addressed. Electronic mail: Ivan.Buijnsters@mtm.kuleuven.be. Tel./Fax: +32 (0)16321233/(0)16321991.

 

engine parts, invasive and implantable medical devices, scratch-resistant glasses and microelectromechanical systems, and ultra-thin DLC foils are being successfully applied to the instrumentation for fusion and space plasma research.[6,12] However, the structure and properties of the a-C:H materials are strongly affected by heat treatment.[13,14] The thermally induced changes in the a-C:H film structure are crucial for these practical applications and the thermal stability of a-C:H films with different microstructure has therefore been studied repeatedly over the last two decades. For this purpose, many different characterization techniques such as Raman spectroscopy, infrared absorption, differential scanning calorimetry/thermogravimetry, x-ray photoelectron spectroscopy, Auger electron spectroscopy, high resolution transmission electron microscopy, elastic recoil detection analysis (ERDA), and thermal desorption have been employed.[11,15–19]

Walters *et al.*[19] performed a neutron diffraction and infrared absorption study on the structure of a-C:H films (~35 at. % H) and they evidenced a significant structural reorganization up to about 300 °C. Overall, the initial room-temperature amorphous network (a mixture of single bonds and olefinic double bonds) became progressively aromatic, then graphitic as hydrogen is desorbed up to 1000 °C.[19] Recently, Peter *et al.*[11] performed a comparative analysis of the thermal induced gas evolution from a-C:H films deposited from different hydrocarbons using thermal desorption spectroscopy. Interestingly, they found the effused gases and the threshold temperatures for gas effusion to be related to the a-C:H structure with the film hardness as a measure—independent of the hydrocarbon precursor.[11]

Until now, the exact mechanism of the thermally activated release of hydrogen and hydrocarbon molecules from a-C:H films remains unclear, but several different models have been discussed repeatedly. Wild and Koidl[20] indicated that the evolution of hydrogen is not limited by a diffusion process, but hydrogen and hydrocarbon species desorb from the edges of the $sp^2$ clusters and effuse rapidly through a network of boundaries decorated by hydrocarbons. Ralchenko *et al.*[21] suggested delocalization of hydrogen atoms followed by surface recombination into hydrogen molecules as the mechanism of $H_2$ release. On the other hand, Gerstenberg and Grischke[22] speculated on the thermally activated rupture of neighboring bonds of network modifiers (-H, $-CH_3$) to the carbon network, the reconstruction of broken carbon bonds and finally the formation of a hydrogen and/or hydrocarbon molecule in the formation of released molecules.[11]

In this study, the stability of H in a-C:H films with tailored microstructure is discussed. X-ray absorption near-edge spectroscopy[23] (XANES) and ERDA were used to study the local-order structural evolution around C sites and the residual H content, respectively. More specifically, the impact of annealing and radiation exposure on the H content is investigated for (soft) polymer-like and (hard) diamond-like carbon films grown on grounded and biased (-200 V) substrates, respectively. Under these growth conditions, a strong variation in the structure and, subsequently, physical properties of the deposited films is attained.[24–27] The H stability provides relevant information about the strength of H bonding in H containing structures, which can be used to unveil the remarkable different mechanical properties displayed by both structures.

## II. EXPERIMENTAL

### A. Sample preparation

a-C:H films were grown by electron-cyclotron-resonance chemical vapor deposition (ECR-CVD) using a two-zone vacuum chamber reactor (ASTEX, model AX4500) operating with a 2.45 GHz microwave source at 208–210 W input power. Double-side polished p-type Si(100) substrates with a thickness of 280 $\mu$m were used. Gas mixtures of $CH_4$/Ar (15/35 cubic centimeter per minute at STP) were applied keeping the operating pressure at 1.47 Pa. This gas mixture was chosen to produce (ultra)smooth a-C:H films with relatively high H content under negative biased substrates above 100 eV.[10,28] Further details about the deposition conditions can be found elsewhere.[26]

In order to study films with different structural and mechanical properties,[24–27] two sets of films were grown for 1 hour on grounded and DC biased (−200 V) substrates, respectively. Although no intentional heating was employed, the substrate temperature was evaluated at the end of each deposition run by a thermocouple attached to the substrate holder. Maximum substrate temperatures of 65 °C and 96 °C and average thickness of the as-grown films of about 800 and 1100 nm were recorded for a-C:H film growth on grounded and biased substrates, respectively. Samples grown under identical conditions were further annealed under high-vacuum conditions ($< 10^{-4}$ Pa) for 1 hour at temperatures of 150 °C, 250 °C, 350 °C, and 450 °C.

### B. Sample characterization

The film composition was derived from ion beam analysis (IBA) techniques. In particular, simultaneous Rutherford backscattering spectrometry (RBS) and ERDA measurements were performed. The spectra were acquired by using a 2 MeV $He^+$ beam impinging at an incidence angle of 75° with respect to the surface normal. The backscattered projectiles and recoil atoms were detected using silicon surface barrier detectors located at scattering angles of 170° and 30°, respectively. In front of the forward detector, a 13 microns thick Mylar foil was placed to filter the H recoils from heavier particles. Both RBS and ERDA experimental spectra have been fitted using the same film structure by the SIMNRA code.[29] The cross-section for the $^1H(\alpha,p)^4He$ process given by Quillet *et al.*[30] was used for quantification of the ERDA yield. The H stability upon ion irradiation of the different annealed structures was further studied from the H loss during the ERDA measurements. For this purpose, measurements steps with a partial charge of 0.25 $\mu$C were acquired up to a total dose of 5 $\mu$C.

XANES measurements were carried out at the dipole beamline PM4 using the SURICAT endstation of the synchrotron facility BESSY-II in Berlin, Germany. The samples were oriented with respect to the incident beam near the 55°

magic angle in order to avoid geometrical effects in the absorption intensity. The data were acquired in the total electron yield (TEY) mode by recording the current drained to ground from the sample. Intensities were normalized to the signal recorded simultaneously from a gold covered grid. The resonance $\pi^*$ peak from highly oriented pyrolytic graphite (HOPG) at 285.4 eV was used for energy calibration at the C(1*s*) edge.

## III. RESULTS AND DISCUSSION

### A. Elastic recoil detection analysis (ERDA)

Fig. 1 shows the scattered yield of H recoils after 0.25 $\mu$C irradiation with 2 MeV $He^+$ ions from the a-C:H samples grown on grounded (a) and biased (b) substrates and post-annealed at different temperatures. The highest energy of detected H recoils corresponds to scattering events at the sample surface whereas those detected at lower energies (channels) provide information about in-depth H distribution. Particularly, the observed yield is a function of the in-depth concentration, scattering cross-section for the projectile energy at each event, and the energy loss of the recoils through the Mylar foil (higher for lower recoil energy). Note that, although the yield decreases at lower energy channels, the H content is homogeneously distributed in depth as derived from simulations of the spectra with the SIMNRA code (not shown).

The ERDA spectra clearly show that the H content in the films grown with grounded substrates is higher than in the case of biasing. Fitting of the ERDA spectra simultaneously with the C signal from RBS results in H contents of ~45 and ~33 at. %, respectively. This implies a relatively

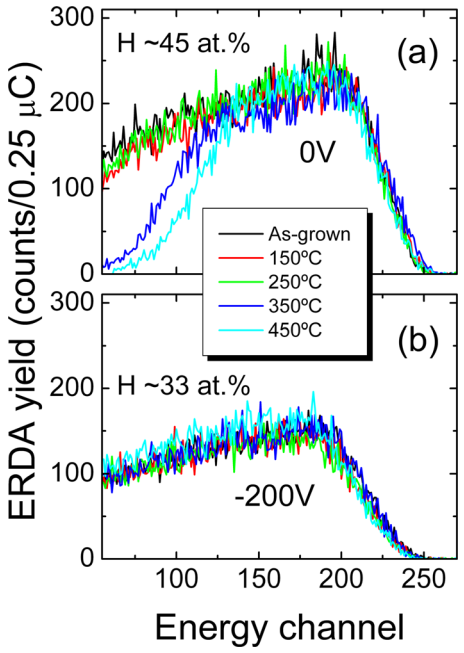


FIG. 1. ERDA spectra for a-C:H films grown by ECR-CVD on (a) grounded and (b) biased substrates. Note the different yield in both cases corresponding to H contents of ~45 at. % (a) and ~33 at. % (b). The impact of annealing only results in a slight decrease in the H content (few at. %) in both cases. For the film with the larger H content (a), the thickness decreases for annealing temperatures above 250 °C.

large amount of H in both structures. Furthermore, in both cases, the H content is not significantly affected with annealing temperatures within the temperature window (up to 450 °C) sampled in this work and only a small decrease of a few at. % has been detected (not very significant considering the sensitivity of the technique). This is in line with the previously recorded starting temperatures for molecular hydrogen effusion in the range 450–600 °C for a-C:H films grown with different hydrocarbon precursors.[11] Despite of this, there is a thickness reduction of the films grown on grounded substrates for annealing temperatures of 350 °C and 450 °C, which has been further verified by the thickness values extracted from spectroscopic ellipsometry (not shown). This indicates that some thermal-induced desorption of the deposited material takes place (note that the thickness modification does not affect significantly the H content in the remaining part). In this respect, Peter *et al.*[11] recently showed that, when heated, a-C:H films release mainly molecular hydrogen, but also oxygen-containing gases such as $H_2O$, CO, and $CO_2$ were measured in substantive quantities. Water vapor is even the second dominant gas and its evolution typically exceeds the hydrocarbon signals.[11,31] In addition, the threshold temperature for the effusion of argon from a-C:H films deposited from hydrocarbon-argon mixtures and softer than 13 GPa was found to be lower than that of the release of molecular hydrogen. Our films were synthesized from an argon-rich methane gas mixture, but RBS data show that only a very limited number of argon ions (<1 at. %) is finally trapped within these films.[24] Nevertheless, argon effusion is related to the changes and the size and number of micropores in a-C:H films.[11] The cauliflower-like surface morphology,[10] higher hydrogen content, and relatively low hardness[26] (~2 GPa) of the a-C:H films deposited on grounded substrates indicate a porous and low-density as-deposited a-C:H film structure with a weakly cross-linked hydrocarbon network. After intermediate exposure to air, this porosity likely has led to a large uptake of water and oxygen molecules that chemically react with the a-C:H material upon annealing.[32] Together with a relatively easy release of argon, this could explain the thickness shrinkage of the a-C:H films grown with grounded substrate for annealing temperatures above 250 °C.

Additional information about the H stability can be extracted from the changes in the ERDA yield with exposure time. For this purpose, ERDA and RBS spectra were acquired after sequential dose steps of 0.25 $\mu$C and up to a total dose of 5 $\mu$C. The ERDA yield normalized to the initial value as a function of the dose is plotted in Fig. 2. In this case, a considerable H loss upon irradiation is present in the films grown on grounded substrates (0 V), indicating that H is weakly bonded to the C matrix. The loss rate is similar for all the samples annealed at different temperatures except for that at 450 °C. This result points out that the same release mechanism (or bonding configuration) takes place for all annealed samples except for the highest temperature where the residual or modified H bonds become slightly stronger in this case. On the contrary, the films grown on biased substrates (−200 V) show a remarkable stability during irradiation, pointing out a very stable H configuration within the C matrix. These

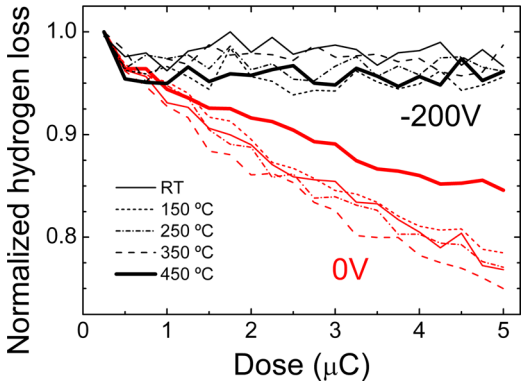


FIG. 2. Normalized H loss rate during ERDA measurements for a-C:H films grown by ECR-CVD on grounded (lower graphs) and biased (upper graphs) substrates. The H loss is noticeable in the case of no substrate biasing, indicating weak H bonding. Note that the loss rate is reduced above 350 °C in such films. In the case of biased growth, the H content is stable during irradiation (within experimental errors) indicating stable C-H arrangements.

observations confirm the results obtained in previous works[33,34] showing that soft polymeric films are prone to large migration of hydrogen under ion beam irradiation as well as decomposition of its hydrocarbon constituents on thermal annealing. Consequently, the amount of carbon in terminal $–CH_3$ groups decreases at the expense of more connective $–CH_2–$ environments during hydrogen depletion due to energetic ion bombardment.[34] The ion-beam induced release of hydrogen is caused by bond breaking due to the secondary electron emission along the ion track and formation of a $H_2$ molecule within a small recombination volume.[34]

### B. X-ray absorption near-edge structure (XANES)

In order to verify structural changes in the C matrix and C-H environments upon annealing, XANES analysis has been performed in the as-grown and annealed samples. Fig. 3 shows the C(1*s*) XANES spectra of as-grown a-C:H films deposited on grounded (0 V) and biased (−200 V) substrates. The signal has been normalized to the maximum of intensity and shifted vertically for comparison purposes. The spectra of graphite and diamond are also shown as reference of pure $sp^2$ and $sp^3$ crystalline materials together with that of an evaporated amorphous carbon (e-C) film as reference for a disordered all-$sp^2$ (∼90%) structure.[35]

Generally, XANES spectra of a-C materials display a two-edge structure with a low-energy edge starting at ∼284 eV associated to $1s \rightarrow \pi^*_{C\text{-}C}$ states from $sp^2$ hybrids and a high-energy edge related to $1s \rightarrow \sigma^*_{C\text{-}C}$ transitions from both $sp^3$ and $sp^2$ hybrids. The position of the $\pi^*$ resonance provides information about the arrangement of $sp^2$ networks.[36] In particular, values below that of graphite (285.4 eV) around ∼285 eV indicate the presence of disordered $sp^2$ hybrids (e.g., see the spectrum of e-C) in chain or ring structures whereas a transition towards the value of graphite reveals the ordering of $sp^2$ clusters into aromatic rings. The onset of the $\sigma^*$ edge shifts from 288 to 290 eV as the amount of $sp^3$ hybrids in the matrix decreases. Normally, the $\sigma^*$ states present a broad structure due to the superposition of different $sp^2$ and $sp^3$ arrangements and atomic intermixing.[37,38] Additional features appear in the case of hydrogenated structures. In the case of H in chain-like structures as in polyethylene ($[\text{-}CH_2\text{-}CH_2\text{-}]_n$), the spectra display a sharp feature at ∼288 eV related to $1s \rightarrow \sigma^*_{C\text{-}H}$ transitions and a broad band at ∼293 eV due to $1s \rightarrow \sigma^*_{C\text{-}C}$.[39] On the other hand, H bonded to C atoms in aromatic rings such as in benzene display a C(1*s*) with two $\pi^*$ (an intense peak at 285 eV and another sharp one at 288.8 eV) and several $\sigma^*$ (293.3 and 300.3 eV) features.[23] The contribution of several H environments within the a-C network on the density of states has been studied theoretically by Robertson *et al.*[40]

Two main features can be identified in the spectra of a-C:H films grown by ECR-CVD, as is indicated in Fig. 3. The first feature at about 285 eV is related to $1s \rightarrow \pi^*_{C\text{-}C}$ transitions, whereas the intensity around 288 eV can be assigned to $1s \rightarrow \sigma^*_{C\text{-}H}$. It should be noted that the signal from C-H bonds presents a broad contribution between 286 and 290 eV.[41] The origin of the minor peak at about 287 eV is not clear but it could be related to some intermixing of $sp^2$ and $sp^3$ C hybrids.

The different spectral shape for the as-grown samples is a clear indication of the structural changes induced by energetic particle bombardment during growth through substrate biasing. In particular, the as-grown sample deposited on grounded substrates presents a PLCH structure. This statement can be extracted by the large contribution of C-H bonds (note the pronounced intensity around 288 eV) and the reduced content of $sp^2$ hybrids (i.e., low signal of the $\pi^*_{C\text{-}C}$ peak). In the case of substrate biasing, the film has a higher content of $sp^2$ hybrids derived by the filling of states in the 286–287 eV region and a lower contribution of C-H around 288 eV. Although the high H content precludes a precise calculation of the $sp^2$ content in the film, an estimate can be derived by using the method described by Gago *et al.*[35] The calculation is based on the comparison of the relative intensity of $\pi^*$ to $\sigma^*$ states with respect to the reference spectrum of e-C (∼90% $sp^2$-C) in Fig. 3. In this case, the integration has been performed between 280–287 eV and 292–303 eV regions of $\pi^*$ to $\sigma^*$ states, respectively, in order to avoid the influence of C-H states. This computation yields a value of ∼55% $sp^2$ C hybrids. Therefore, this film can be catalogued as DLCH according to the criteria of Casiraghi *et al.*[4]

The C-H band in the XANES spectra for PLCH and DLCH films has been highlighted in Fig. 3. It should be noted that the intensity of such bands does correlate with the H contents extracted from ERDA. In an earlier publication,[24] it was pointed out that the non-proportional relation between ERDA and XANES intensities could be explained from the presence of H atoms not bonded to C. It is expected that the number of such H atoms is higher in PLCH films, which results in the inferior stability of H in such structure. Another contribution could come from different bonding environments for each structure with different sensitivity factors (X-ray absorption cross-section). In particular, the low $sp^2$ content in PLCH suggests the dominance of saturated (weak) C-H bonds in chain-like structures, whereas H is presumably incorporated in (stable) terminating bonds within the C matrix in DLCH. Both assumptions correlate well with the low (high) stability of PLCH (DLCH) films upon MeV $He^+$

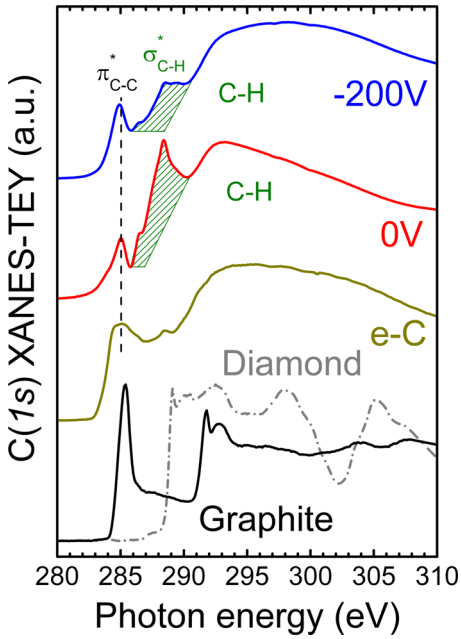


FIG. 3. XANES spectra of a-C:H films grown by ECR-CVD on grounded and biased substrates. The spectra of graphite and diamond have been included as reference of pure $sp^2$ and $sp^3$ crystalline materials, respectively. The spectrum of evaporated (amorphous) carbon, labelled as e-C, is also included as a reference material of disordered $sp^2$ (~90%) structures.

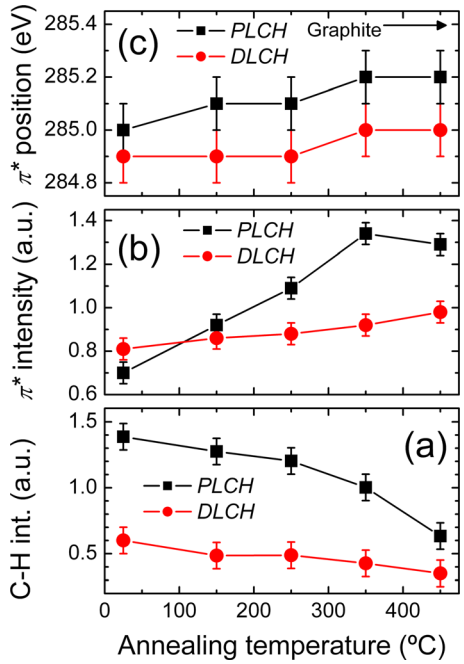


FIG. 5. Evolution of XANES spectral features with annealing temperature for PLCH (■) and DLCH (●) films: (a) C-H intensity, (b) $\pi^*$ intensity, and (c) $\pi^*$ position. The reference energy corresponding to the $1s \rightarrow \pi^*_{C-C}$ transition in graphite is indicated in (c).

irradiation (Fig. 2). This hypothesis is further discussed below.

The evolution of the XANES spectrum with annealing temperature for as-grown PLCH (0 V) and DLCH (−200 V) films is shown in Fig. 4. In both cases, a clear decrease in the C-H intensity (label C3) takes place, which is shown quantitatively in Fig. 5(a). The impact is more pronounced in PLCH, especially above 350 °C. This trend correlates with the major changes observed in the ERDA profiles of Fig. 1 (i.e., thermal desorption and thickness decrease). However, ERDA did not show such a significant H decrease, suggesting that strong structural modifications and H-loss occur mainly at the near-surface region of the samples upon annealing (while keeping the bulk properties in terms of H concentration mainly unaltered). An additional common feature in both types of films is a graphitization process (i.e., promotion of $sp^2$ hybrids). This transformation is derived from the progressive increase in the $\pi^*$ intensity and the shift of the $\pi^*$ resonance towards the value of graphite (285.4 eV). Both trends are displayed in Figs. 5(b) and 5(c), respectively. As in the case of the C-H signal, the changes are more severe for PLCH where the final configuration is more similar to graphite than in DLCH. This trend is an additional confirmation of the high thermal stability of the DLCH structure. It also points out that the aromatic rings in PLCH (shift of ~0.2 eV in the $\pi^*$ resonance position) are formed by structural transformation after release of weakly bonded H. In the case of DLCH, the graphitization process is partially inhibited by the high H stability which precludes the development of dangling bonds that would collapse into aromatic rings.

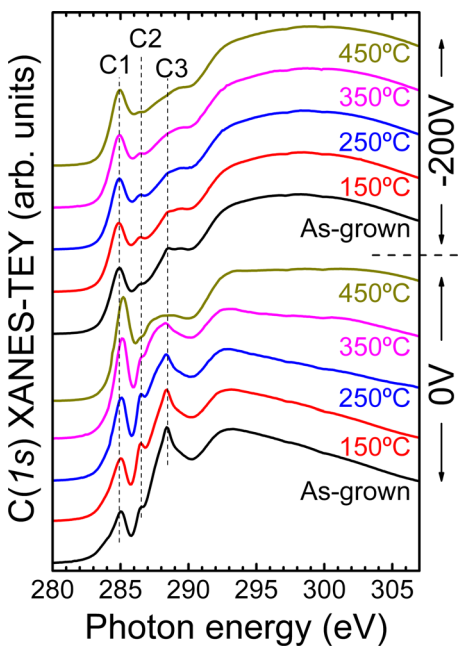


FIG. 4. Evolution of the XANES spectra upon annealing for PLCH (lower curves) and DLCH (upper curves) films grown on grounded (0 V) and biased (−200 V) substrates, respectively. Positions corresponding to (local) maximum intensity of the $1s \rightarrow \pi^*_{C-C}$ and $1s \rightarrow \sigma^*_{C-H}$ transitions are labelled C1 and C3.

In order to study the different C-H bonding configurations in PLCH and DLCH, Fig. 6 shows the C-H contribution to the XANES spectra after subtraction of the background imposed by the $\sigma^*$ edge. The intensity of the signal was used for the quantification shown in Fig. 5(a). In general, the XANES signal in the range from 286 eV to 290 eV is ascribed to a single C-H band. However, the presence of multiple C-H bonding states gives rise to a complex band structure, as is the case for the multiple bonding geometries corresponding to carbon $sp^2$ hybrids forming $\pi$ and $\sigma$

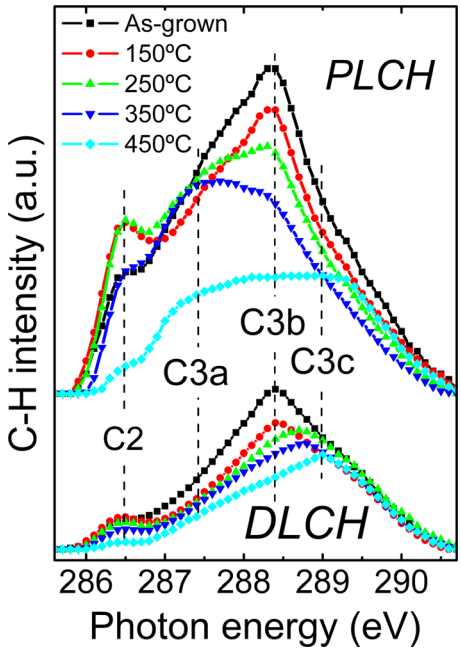


FIG. 6. Evolution of the XANES spectral intensity related to C-H bonding configurations for PLCH (upper curves) and DLCH (lower curves) grown on grounded (0 V) and biased (−200 V) substrates. Positions corresponding to (local) maximum C-H intensity at different annealing temperatures are labelled C2, C3a, C3b, and C3c.

bonds.[37] It is noteworthy that both signals for as-grown samples (Fig. 6) display a maximum around C3b, indicating a similar starting configuration. However, the intensity in PLCH shifts towards lower energies (C3a) at intermediate temperature and another contribution appears at higher energy (C3c) as the annealing temperature is further increased. The intensity in DLCH also shifts gradually from C3b to C3c as the annealing temperature is increased. In addition, there is a clear signal at about 286.5 eV (C2) for both types of films which decreases in intensity with annealing temperature.

The different components in the C-H band originate from variations in the number of H atoms per C atom and differences in the bonding configuration of the C atom itself, i.e., $sp^2$-trigonal vs. $sp^3$-tetragonal. This has been observed for the case of well-defined bonding environments in $C_6$-ring molecules, which depending on the number of double bonds within the molecule exhibit significant variations in the XANES C-H band from increased intensity at higher energies in benzene (i.e., one H per C atom) to dominance of the band at lower energies in cyclohexane (i.e., two H per C atom).[42] When dealing with solids instead of isolated molecules, the shape of the C-H band is also sensitive to the degree of order beyond first neighbors, as has been shown for the case of polyethylene chains with different number of lateral branches.[43] In the case of our a-C:H films, the situation is even more complex, since a mixture of alkane chains and different C-ring sizes is present, and it is difficult to make a direct assignment of the observed features. Nevertheless, in accordance with Refs. 42 and 43, the XANES trends suggest a transition from alkane and non-aromatic carbon sites towards more graphitic (benzene-like) environments.

## IV. CONCLUSIONS

We have shown that a-C:H films with PLCH and DLCH structures can be grown by ECR-CVD on grounded and biased substrates, respectively. PLCH films are unstable upon annealing and against swift-ion irradiation since they suffer desorption above 350 °C and the hydrogen out-diffuses during ERDA measurements. Remarkably, PLCH annealed to the highest annealing temperature of 450 °C shows an improvement in radiation resistance. On the other hand, DLCH structures are quite stable upon annealing up to 450 °C and during swift-ion irradiation. The evolution of the C(1*s*) XANES edge reveals a graphitization process upon annealing in both types of films. However, the strong H loss in PLCH drives to the formation of aromatic clusters due to the collapse of the C matrix, whereas the higher H stability of DLCH reduces the degree of graphitization.

## ACKNOWLEDGMENTS

We acknowledge the HZB-BESSY II for provision of synchrotron radiation at beamline PM4 and thank A. Völlmer for technical assistance. This research has been funded from the EC's FP7/2007-2013 under Grant No. 226716 and from the Spanish "*Ministerio de Ciencia e Innovación*" through Grant Nos. FIS2009-12964-C05-04, CSD2008-00023, and MAT2010-21070-C02-02. A.R.C. acknowledges funding from SFRH/BPD/74095/2010 (Portugal), and J.G.B. would like to thank the Executive Research Agency of the European Union for funding under the Marie Curie **IEF** Grant No. 272448.

[1]T. C. Arnoldussen and E. M. Rossi, Ann. Rev. Mater. Sci. **15**, 379 (1985).
[2]J. Robertson, Mater. Sci. Eng. R. **37**, 129 (2002).
[3]R. Hauert and U. Müller, Diamond Relat. Mater. **12**, 171 (2003).
[4]C. Casiraghi, A. C. Ferrari, and J. Robertson, Phys. Rev. B **72**, 085401 (2005).
[5]A. Erdemir, M. Switala, R. Wei, and P. Wilbur, Surf. Coat. Technol. **50**, 17 (1991).
[6]A. Erdemir and C. Donnet, J. Phys. D: Appl. Phys. **39**, R311 (2006).
[7]C. Hopf, W. Jacob, and A. von Keudell, J. Appl. Phys. **97**, 094904 (2005).
[8]I. Ahmad, S. S. Roy, P. D. Maguire, P. Papakonstantinou, and J. A. McLaughlin, Thin Solid Films **482**, 45 (2005).
[9]M. Moseler, P. Gumbsch, C. Casiraghi, A. C. Ferrari, and J. Robertson, Science **309**, 1545 (2005).
[10]J. G. Buijnsters, M. Camero, and L. Vázquez, Phys. Rev. B **74**, 155417 (2006).
[11]S. Peter, M. Günther, and F. Richter, Vacuum **86**, 667 (2012).
[12]V. Liechtenstein, V. Jaggi, E. Olshanki, J. A. Scheer, P. Wurz, and S. K. Zeisler, Nucl. Instrum. Meth. Phys. Res. A **613**, 429 (2010).
[13]R. Kalish, Y. Lifshitz, K. Nugent, and S. Prawer, Appl. Phys. Lett. **74**, 2936 (1999).
[14]S. Takabayashi, K. Okamoto, H. Sakaue, T. Takahagi, K. Shimada, and T. Nakatani, J. Appl. Phys. **104**, 043512 (2008).
[15]C. Louro, C. Wagner Moura, N. Carvalho, M. Stueber, and A. Cavaleiro, Diamond Relat. Mater. **20**, 57 (2011).
[16]W. S. Choi and B. Y. Hong, Renewable Energy **33**, 226 (2008).
[17]R. L. C. Wu, K. Miyoshi, R. Vuppuladhadium, and H. E. Jackson, Surf. Coat. Technol. **54–55**, 576 (1992).
[18]D. R. Tallant, J. E. Parmeter, M. P. Siegal, and R. L. Simpson, Diamond Relat. Mater. **4**, 191 (1995).
[19]J. K. Walters, D. M. Fox, T. M. Burke, O. D. Weedon, R. J. Newport, and W. S. Howells, J. Chem. Phys. **101**, 4288 (1994).
[20]C. Wild and P. Koidl, Appl. Phys. Lett. **51**, 1506 (1987).
[21]V. G. Ralchenko, E. N. Loubnin, A. V. Popov, and V. E. Strelnitsky, Diamond Relat. Mater. **1**, 345 (1992).
[22]K. W. Gerstenberg and M. Grischke, J. Appl. Phys. **69**, 736 (1991).

[23]J. Stöhr, *NEXAFS Spectroscopy* (Springer-Verlag, New York, 1992).
[24]J. G. Buijnsters, R. Gago, I. Jiménez, M. Camero, F. Agulló-Rueda, and C. Gómez-Aleixandre, J. Appl. Phys. **105**, 093510 (2009).
[25]J. G. Buijnsters, M. Camero, R. Gago, A. R. Landa-Canovas, C. Gómez-Aleixandre, and I. Jiménez, Appl. Phys. Lett. **92**, 141920 (2008).
[26]J. G. Buijnsters, M. Camero, L. Vázquez, F. Agulló-Rueda, R. Gago, I. Jiménez, C. Gómez-Aleixandre, and J. M. Albella, Diamond Relat. Mater. **19**, 1093 (2010).
[27]J. G. Buijnsters, M. Camero, L. Vázquez, F. Agulló-Rueda, C. Gómez-Aleixandre, and J. M. Albella, Vacuum **81**, 1412 (2007).
[28]J. G. Buijnsters and L. Vázquez, Surf. Coat. Technol. **201**, 8950 (2007).
[29]M. Mayer, SIMNRA User's Guide, IPP Report 9/113 (Max Planck Institute, Garching, Germany, 1997).
[30]V. Quillet, F. Abel, and M. Schott, Nucl. Instrum. Meth. B **83**, 47 (1993).
[31]A. Schenk, B. Winter, J. Biener, C. Lutterloh, U. A. Schubert, and J. Küppers, J. Appl. Phys. **77**, 2462 (1995).
[32]V. Kulikovsky, V. Vorlíček, P. Bohác, A. Kurdyumov, and L. Jastrabík, Thin Solid Films **447–448**, 223 (2004).
[33]M. E. Adel, O. Amir, R. Kalish, and L. C. Feldman, J. Appl. Phys. **66**, 3248 (1989).
[34]T. Som, M. Malhotra, V. N. Kulkarni, and S. Kumar, Phys. B **355**, 72 (2005).
[35]R. Gago, I. Jiménez, J. M. Albella, A. Climent-Font, D. Cáceres, I. Vergara, J. C. Banks, B. L. Doyle, and L. J. Terminello, J. Appl. Phys. **87**, 8174 (2000).
[36]R. Gago, M. Vinnichenko, H. U. Jäger, A. Yu. Belov, I. Jiménez, N. Huang, H. Sun, and M. F. Maitz, Phys. Rev. B **72**, 14120 (2005).
[37]I. Jiménez, R. Gago, and J. M. Albella, Diamond Relat. Mater. **12**, 110 (2003).
[38]J. Diaz, O. R. Monteiro, and Z. Hussain, Phys. Rev. B **76**, 094201 (2007).
[39]Y. Wang, Y. Zou, T. Araki, J. Lüuning, A. L. D. Kilcoyne, J. Sokolov, H. Ade, and M. Rafailovich, Macromolecules **43**, 8153 (2010).
[40]J. Robertson and E. P. O'Reilly, Phys. Rev. B **35**, 2946 (1987).
[41]R. Gago, I. Jiménez, and J. M. Albella, Surf. Sci. **482**, 530 (2001).
[42]C. Kolczewski, R. Püttner, M. Martins, A. S. Schlachter, G. Snell, M. M. Sant'Anna, K. Hermann, and G. Kaindl, J. Chem. Phys. **124**, 034302 (2006).
[43]A. Schöll, R. Fink, E. Umbach, G. E. Mitchell, S. G. Urquhart, and H. Ade, Chem. Phys. Lett. **370**, 834 (2003).